

Ag-induced a New Raman Mode in ZnO Microrods

Lina WANG^{1,2}, Jing WANG^{2*}, Meina WANG³, Dan ZHOU², Yan MEI², Wenzhuo HUANG², Tian XING², Shengxu GE², Yuntong CHEN², You YU², Zhongqi LUAN², Bing QU², Yaxiang BAI², Chao PAN², Delong TANG², Na ZHU², Yu QIU¹, Lizhong HU¹

¹ School of Physics and Optoelectronic Technology, Dalian University of Technology, Dalian 116024, China

² Key Laboratory of Marine Biophysics of Liaoning Province, Dalian Ocean University, Dalian 116023, China

³ Educational Technology Center, Shenyang Medical College, Shenyang 110034, China

crossref <http://dx.doi.org/10.5755/j01.ms.25.3.19130>

Received 27 September 2017; accepted 13 April 2018

The chemical vapor deposition technique was used to prepare the Ag doped ZnO microrods, which were located on Si substrates at two different positions. The scanning electron microscopy revealed that the samples have a clear hexagonal shape. X-ray diffraction provided information about the preferential orientation along the c-axis. The Raman analysis revealed that a new Raman mode appears at 492 cm⁻¹ due to Ag doping. As this mode has not been reported early, it could be used as a characteristic mode of Ag doping in Raman spectrum. The red shift of the E₂ (high) mode proves the existence of tensile stress in the samples.

Keywords: ZnO microrods, Ag doping, Raman spectrum.

1. INTRODUCTION

Because of the wide band gap and relatively large exciton binding energy, ZnO has stimulated a range of research interests for short wavelength optoelectronic devices [1], surface acoustic waveguides [2], solar cells [3], gas sensors [4], and some piezoelectric devices [5]. There has been a lot of efforts to find out the physical, optical, and electrical properties of nano structures, even in the applications in constructing micro-nano scale electronic or optoelectronic devices. To date, many ZnO nanostructures have been constructed, such as nanorods, nanotubes, nanoplates, nanonails, and nanowires. Many dopants, such as Ag and Cu, have been used to adjust the properties of ZnO nanostructures [6, 7]. As an element of group-IB, Ag can act as acceptor in ZnO, which can occupy the substitutional Zn or the interstitial sites [8].

The properties of the doped ZnO micro-nanostructures are strongly dependent upon the deposition method, doping elements, substrate, and intrinsic defects [9]. Many synthesis techniques are applied to prepare doped ZnO, such as the electrochemical solution method [10], modified thermal-evaporation process [11], aqueous-based chemical method [12], and chemical vapor deposition [13]. The chemical vapor deposition (CVD) method is a much simpler technique under stable and reproducible conditions when compared to the other techniques [14]. Furthermore, the Raman scattering technique is a non-destructive and valuable test to study the phonon behavior of doped ZnO materials. It can also provide the lattice dynamics, defects, and information of the crystal structure.

In this paper, the Ag doped ZnO microrods (AZMR) were synthesized by Chemical Vapor Deposition (CVD) method on Si substrates. The influence of Ag elements on morphologies and Raman properties were thoroughly

studied. Raman spectra reveals that due to Ag doping there is a vibrational mode at 492 cm⁻¹, which has not been reported by other researchers.

2. EXPERIMENTAL DETAILS

The horizontal tube furnace equipment was used to deposit the AZMR on Si substrate by the CVD method. The CVD system was composed of three parts: a gas controller, a temperature control system, and a horizontal tube furnace. Fig.1 shows the illustration of the experimental system. A mixture powder of ZnO (2 g), graphite (0.4 g), and Ag₂O (2 g), which each act as a reaction source, were placed at one end of a quartz tube (diameter 3 cm, length 35 cm). The two Si substrates were placed downstream of the mixture powders, with sample a being placed 10 cm away from the mixture powders and sample b being placed 30 cm away.

While amidst a mixture gas of N₂ and O₂ (100 sccm for N₂ and 40 sccm for O₂), the growth temperature of the mixture powders was maintained at a temperature of 950 °C for 60 minutes. The furnace system was chill-down to room temperature with constant flow of N₂ after growth. Subsequently, AZMR was found on the surface of sample a, and Ag doped ZnO micromultiple (AZMM) was found on the surface of sample b.

The morphology of the sample was studied in a Hitachi SU1510 scanning electron microscope (SEM) operating at 20 kV. The energy dispersive X-ray spectroscopy (EDS) attached to the SEM was used to analyze elemental composition. The structural properties were analyzed by X-ray diffraction (XRD; RigakuD/max3B), which was performed in a θ -2 θ configuration. The micro-Raman system (Jobin Yvon LabRAM HR 800UV) was used to characterize the optical properties at room temperature.

* Corresponding author. Tel.: +86-0411-84763979; fax: +86-0411-84709304. E-mail address: l.n.w@163.com (J. Wang)

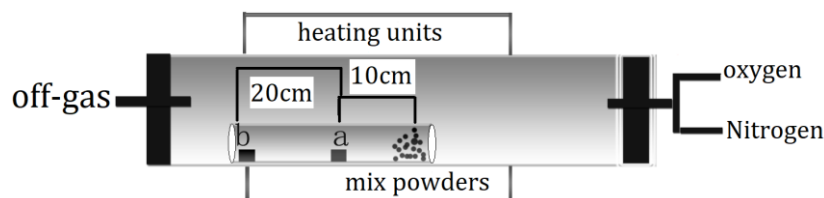


Fig. 1. The illustration of experimental system.

3. RESULTS AND DISCUSSION

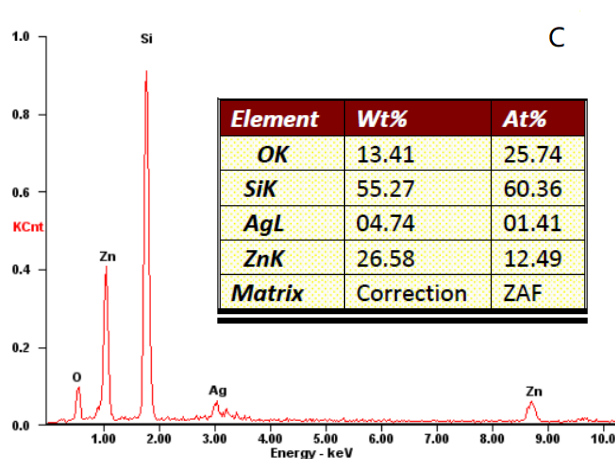
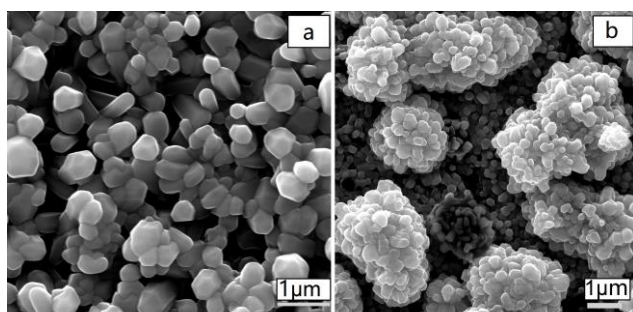


Fig. 2. SEM images of Ag doped ZnO microrods: a–10 cm away from the vapour source; b–30 cm away; c–EDX spectra of sample b

The SEM images of AZMR and AZMM shown in Fig. 2 give a general view of microstructures on the Si substrates. As shown in Fig. 2 a, uniform Ag doped ZnO microrods can be observed with about 400 nm in diameter and up to 700 nm in length. The microrods each move in the vertical direction and are all almost uniform in length and size. Furthermore, the figure shows that the microrods have a clear hexagonal shape with smooth and clean side walls. This hexagonal morphology means that the ZnO microrods have a perfect wurtzite structures. Fig. 2 indicates that the AZMR have a preferential c-axis growth direction, and it was in {100} the hexagonal facet. Fig. 2 b shows the SEM images of sample b, which display the ZnO micromultiple structures. Just as sample a, the base layer is Ag doped ZnO microrods and the top layer is Ag doped lumps-like ZnO micro-nanostructure. Fig. 2 c shows the EDX spectra of sample b, the Ag peak appears at 3.0 keV, which means the Ag successfully doped in the

nanostructures. The mass ratio of Ag and Zn is about 1:5.6. because of the different melting point, only part of the Ag doped in the nanostructure during the whole process.

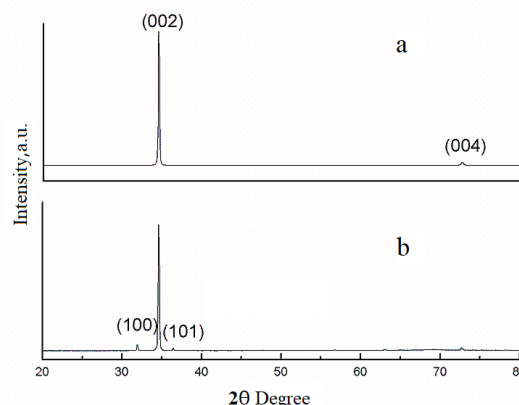


Fig. 3. XRD patterns of sample a and b

The reason for the difference between the two samples can be attributed to the substrate temperature. Sample a is next to the evaporation source, therefore it is in the heating zone and the substrate temperature is high. Sample b is out of the heating zone, leading to a lower substrate temperature than sample a and different morphology between the two samples.

The relationship between temperature and ZnO nanostructures was studied by Wang et al., who believed that two reasons may be responsible for the difference: the changing of ZnO vapor and the different thermal expansion coefficient between the substrate and nanostructures [15].

Fig. 3 shows the XRD patterns of sample a and sample b. Four peaks can be observed: with the Miller indices (hkl), namely (100), (002), (101), (004). For the standard hexagonal ZnO, the 2-theta value of the four peaks were separately located at 31.77°, 34.45°, 36.25°, and 72.56°. Corresponding to ZnO (002) peak, the figure shows that the peaks at about 34.31° and 34.37° are very strong, and aside from ZnO, no phases related to Ag oxides can be observed. This indicates that Ag doped ZnO micro-nanostructures have a hexagonal wurtzite structure and a preferential orientation along the c-axis. Compared to pure ZnO, the (002) peak located at 34.45° has a slight shift to the lower 2θ angle direction. This is primarily because the ionic radius of Ag⁺(122pm) is larger than Zn²⁺(72pm). As a dopant in ZnO, Ag can occupy the interstitial (Ag_i^{*}) or substitutional Zn²⁺ sites Ag_{Zn}['] [8].

The Raman scattering technique is non-destructive and a stable test to study the defects, structural disorder, and

crystalline quality in the doped ZnO micro-nanostructures. It can provide important information about the change of local structure, owing to the incorporation of doped ions. According to the group theory, ZnO single crystal is in the C_{6v} point group symmetry, including two Raman silence B_1 modes and six other Raman phonon modes [16]. The two E_2 modes are divided into high and low frequencies located at 437 and 101 cm^{-1} . The A_1 and E_1 modes are separated into transverse and longitudinal modes. The two A_1 modes are 380 and 574 cm^{-1} , and the two E_1 modes are 407 and 583 cm^{-1} .

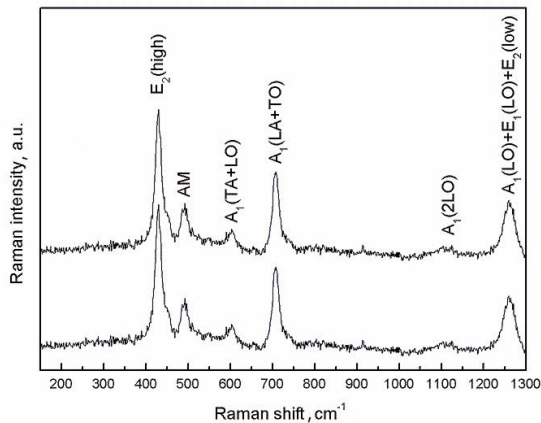


Fig. 4. The Raman spectra of sample *a* and *b*

Fig. 4 shows the Raman scattering of sample *a* and sample *b* over the 100–1300 cm^{-1} range. There are not many other differences between the two samples. The peak at 429 cm^{-1} is E_2 (high) mode, this mode has a strong relationship with the wurtzite structure of ZnO; its intensity indicates the perfect crystallinity. The shift of the E_2 mode provides information about stress: the compressive stress was dominating if shifting in the direction of high frequency, and the tensile stress was dominating when shifting in the other direction [17]. When compared with the stand mode, the E_2 (high) mode of standard ZnO was located at 437 cm^{-1} . An 8 cm^{-1} downshift was observed, which means the two samples both have tensile stress. The second order of Raman peaks with A_1 symmetry (601, 706, 1108 cm^{-1}) can also be observed. The $A_1(\text{LO}) + E_1(\text{LO}) + E_2$ (low) peak was located at 1262 cm^{-1} as a result of the multiple phonon scattering processes. Apart from the peaks mentioned above, the local vibration mode (LVM) at 492 cm^{-1} with strong intense could also be found. The LVMs caused by other dopants were also found, such as Fe, Ga, and Sb doped ZnO films; the LVMs were located at 720, 631, and 531 cm^{-1} , respectively [18]. They believed the LVMs were caused by doped elements and can be used as incorporation indicators. After depositing Ag doped ZnO films on sapphire substrate by pulsed laser deposition, we found a LVM at 492 cm^{-1} , which was induced by Ag doping [19]. Therefore, we presume that the Raman mode at 492 cm^{-1} should be attributed to LVM caused by Ag doping. AZMR, AZMM, and Ag doped ZnO films were each synthesized using different methods on different substrates; both LVMs at 492 cm^{-1} appeared. Thus, this mode should be marked as a symbol of Ag incorporation into the ZnO micro-nanostructures.

4. CONCLUSIONS

In summary, the CVD method was used to synthesize Ag doped ZnO microrods on Si substrates. The SEM results show that the samples have a hexagonal structure and are grown in the preferential *c*-axis direction. The XRD patterns also corroborate the hexagonal wurtzite structure and proves that the samples were growing along the *c*-axis. Raman spectrum portrays the existence of stress in the samples and a characterized Raman mode at 492 cm^{-1} could be indicative of the successful Ag doping in ZnO microstructures. The mechanism that doping with Ag can induce an extra Raman mode may in connection with the location of Ag^+ , further studied can be made to discuss whether it can be represent Ag_i^* or Ag'_{Zn} .

Acknowledgments

This work was supported by the Nature Science Foundation of Liaoning Province (No. 20170540109 and No.201601285).

REFERENCES

1. Qiu, Y., Zhang, H.Q., Hu, L.Z., Wang, L.N., Wang, B., Yang, D.C., Liu, G.Q., Ji, J.Y., Liu, X., Lin, J.F., Lang, Y., Li, F., Han, S.J. Improving the Quality of Schottky Contacts on ZnO Microwires Using Cu-Contained Silver Paste Electrode *Micro & Nano Letters* 7(6) 2012: pp. 592–595. <https://doi.org/10.1049/mnl.2012.0269>
2. Verardi, P., Nastase, N., Gherasim, C., Ghicac, C., Dinescud, M., Dinud, R., Flueraub, C. Scanning Force Microscopy and Electron Microscopy Studies of Pulsed Laser Deposited ZnO Thin Films. Application to the Bulk:Acoustic Waves(BAW) Devices *Journal of Crystal Growth* 197(3) 1999: pp. 523–528. [https://doi.org/10.1016/S0022-0248\(98\)00808-2](https://doi.org/10.1016/S0022-0248(98)00808-2)
3. Rau, U., Schmidt, M. Electronic Properties of ZnO/CdS/Cu (In, Ga) Se-2 Solar Cells Aspects of Heterojunction Formation *Thin Solid Films* 387(1) 2001: pp. 141–146. [https://doi.org/10.1016/S0040-6090\(00\)01737-5](https://doi.org/10.1016/S0040-6090(00)01737-5)
4. Yamazaki, T., Wada, S., Noma, T., Suzuki, T. Gas-sensing Properties of Ultrathin Zinc-Oxide Films *Sensors and Actuators B* 14(93) 1993: pp. 594–595. [https://doi.org/10.1016/0925-4005\(93\)85106-K](https://doi.org/10.1016/0925-4005(93)85106-K)
5. Zhou, J., Gu, Y., Fei, P., Mai, W., Gao, Y. Flexible Piezotronic Strain Sensor *Nano Letters* 8(9) 2008: pp. 3035–3040. <https://doi.org/10.1021/nl802367t>
6. Ren, C.L., Yang, B.F., Wu, M., Xu, J., Fu, Z., Lv, Y., Guo, T., Zhao, Y., Zhu, C. Synthesis of Ag/ZnO Nanorods Array with Enhanced Photocatalytic Performance *Journal of Hazardous Materials* 182(1–3) 2010: pp. 123–129. <https://doi.org/10.1016/j.jhazmat.2010.05.141>
7. Zeferino, R.S., Flores, M.B., Pal, U. Photoluminescence and Raman Scattering in Ag-doped ZnO Nanoparticles *Journal of Applied Physics* 109(1) 2011: pp. 065303. <https://doi.org/10.1063/1.3530631>
8. Bian, H.Q., Ma, S.Y., Zhang, Z.M., Gao, J.M., Zhu, H.B. Microstructure and Raman Scattering of Ag-doping ZnO Films Deposited on Buffer Layers *Journal of Crystal Growth* 394(394) 2014: pp. 132–136. <https://doi.org/10.1016/j.jcrysgro.2014.02.036>

9. **Hu, Z.G., Li, W.W., Wu, J.D., Sun, J., Shu, Q.W.** Optical Properties of Pulsed Laser Deposited Rutile Titanium Dioxide Films on Quartz Substrates Determined by Raman Scattering and Transmittance Spectra *Apply Physics Letters* 93 (18) 2008: pp. 7454.
<https://doi.org/10.1063/1.3021074>
10. **Liang, J.K., Su, H.L., Kuo, C.L., Kao, S.P., Cui, J.W.** Structural, Optical and Electrical Properties of Electrodeposited Sb-Doped ZnO Nanorod Arrays *Electrochimica Acta* 125 (12) 2014: pp. 124–132.
<https://doi.org/10.1016/j.electacta.2014.01.029>
11. **Fan, D.H., Zhang, R., Li, Y.** Synthesis and Optical Properties of Phosphorus-Doped ZnO Nanocombs *Solid State Communications* 150 (39) 2010: pp. 1911–1914.
<https://doi.org/10.1016/j.ssc.2010.07.036>
12. **Panigrahy, B., Aslam, M., Bahadur, D.** Aqueous Synthesis of Mn- and Co-Doped ZnO Nanorods *The Journal of Physical Chemistry C* 114 (27) 2010: pp. 11758–11763.
<https://doi.org/10.1021/jp102163b>
13. **Ding, M., Yao, B., Zhao, D., Fang, F., Shen, D.** The Effect of Arsenic Thermal Diffusion on the Morphology and Photoluminescence Properties of Sub-Micron ZnO Rods *Thin Solid Films* 518 (15) 2010: pp. 4390–4393.
<https://doi.org/10.1016/j.tsf.2010.02.009>
14. **Suh, D.I., Byeon, C.C., Lee, C.L.** Synthesis and Optical Characterization of Vertically Grown ZnO Nanowires in High Crystallinity Through Vapor-Liquid-Solid Growth Mechanism *Applied Surface Science* 257 (5) 2010: pp. 1454–1456.
<https://doi.org/10.1016/j.apsusc.2010.08.067>
15. **Wang, X.H., Li, R.B., Fan, D.H.** Control Growth of Catalyst-Free High-Quality ZnO Nanowire Arrays on Transparent Quartz Glass Substrate by Chemical Vapor Deposition *Applied Surface Science* 257 (7) 2011: pp. 2960–2964.
<https://doi.org/10.1016/j.apsusc.2010.10.100>
16. **Youn, C.J., Jeong, T.S., Han, M.S., Kim, J.M.** Optical Properties of Zn-Terminated ZnO Bulk *Journal of Crystal Growth* 261 (4): 2004: pp. 526–532.
<https://doi.org/10.1016/j.jcrysgro.2003.09.044>
17. **Huang, Y., Liu, M., Li, Z., Zeng, Y., Liu, S.** Raman Spectroscopy Study of ZnO-Based Ceramic Films Fabricated by Novel Sol-Gel Process *Materials Science and Engineering B* 97 (2) 2003: pp. 111–116.
[https://doi.org/10.1016/S0921-5107\(02\)00396-3](https://doi.org/10.1016/S0921-5107(02)00396-3)
18. **Bundesmann, C., Ashkenov, N., Schubert, M., Spemann, D., Butz, T.** Raman Scattering in ZnO Thin Films Doped With Fe,Sb,Al,Ga and Li *Apply Physics Letters* 83 (10) 2003: pp. 1974–1976.
<https://doi.org/10.1063/1.1609251>
19. **Wang, L.N., Hu, L.Z., Zhang, H.Q., Qiu, Y., Lang, Y.** Studying The Raman Spectra of Ag Doped ZnO Films Grown by PLD *Materials Science in Semiconductor Processing* 14 (3–4) 2012: pp. 274–277.
<https://doi.org/10.1016/j.mssp.2011.05.004>